Technion - Israel Institute of Technology

Robust Guidance and Control (038781)

Spring 2018

Project 3
3D Non-Linear Vector Guidance

Prof. Shaul Gutman

By : Daniel Engelsman, 300546173

August 16, 2018

Contents

List of Figures

Chapter A - 3D Exo-Atmospheric Interception Under Limited Controllers

1 Kinematics, Guidance, and Optimal Strategy

As seen on the course book, when considering 2 vehicles (**P** - Pursuer, **E** - Evader) moving in an exo-atmospheric space, denoted as ($\mathbf{r}_i$ - position, $\mathbf{v}_i$ - velocity). Relatively :

$$r = r_E - r_P \tag{1.1}$$

$$v = v_E - v_P \tag{1.2}$$

$$Assuming \quad g_E \simeq g_P, \quad we \quad get:$$

$$\ddot{r} = \ddot{r}_E - \ddot{r}_P = (w + g_E) - (u + g_P) = w - u \tag{1.3}$$

$$\dot{r} = v \tag{1.4}$$

$$\dot{v} = w - u \tag{1.5}$$

Assuming ideal conditions, using the state vector $\mathbf{x} = [\text{ r} \quad \text{v }]^T$ we get state space :

$$\dot{x} = Ax + Bu + Cv \quad ; \quad Respectively: \tag{1.6}$$

$$\dot{x} = \begin{bmatrix} 0 & I_3 \\ 0 & 0 \end{bmatrix} x + \begin{bmatrix} 0 \\ -I_3 \end{bmatrix} u + \begin{bmatrix} 0 \\ I_3 \end{bmatrix} w \tag{1.7}$$

Guidance Problem

Let us associate the terminal set :

$$\tau = \{x : \|r\| = \|r_E - r_P\| = \big\|[I_3 \quad 0]x\big\| \leq m\} \tag{1.8}$$

As developed comprehensively in **project 2**, we solved the differential game conflict assuming $J^* = \big\|y^*(0)\big\| = m$, ending up with the optimal trajectory plane in ($\|y\|$, t_{go}) :

$$\big\|y^*(t_{go})\big\| = \big\|r + t_{go}v\big\| = m + \frac{1}{2}\Delta\rho t_{go}^2 \tag{1.9}$$

Graphically speaking :

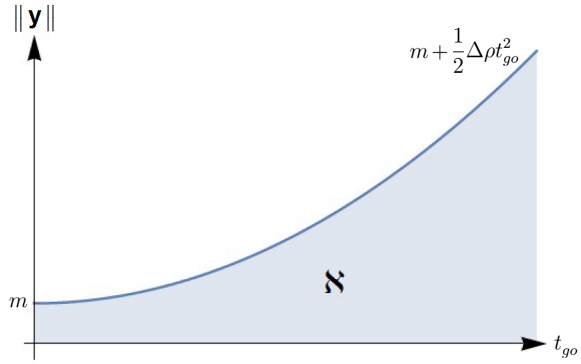

Figure 1: State Space Decomposition: Fixed t_f

Developing (**Eq.** 1.9)^2, would lead us into 4th order polynomial :

$$\frac{1}{4}\Delta\rho^2 t_{go}^4 + (m\Delta\rho - \|v\|^2)\cdot t_{go}^2 - 2(r^T v)\cdot t_{go} + (m^2 - \|r\|) = 0 \tag{1.10}$$

That its smallest root will be the optimal strategies pair $\{u^*, w^*\}$ in inertial coordinates :

$$\mathbf{u}^* = \begin{cases} \rho_u \cdot \dfrac{\mathbf{r}+t_{go}\mathbf{v}}{\|\mathbf{r}+t_{go}\mathbf{v}\|} & \textit{Outside } \aleph \\ \|\mathbf{r}+t_{go}\mathbf{v}\| - m - \dfrac{1}{2}\Delta\rho\cdot t_{go}^2 = 0 & \text{Arbitrary in } \aleph \end{cases} \qquad \mathbf{w}^* = \begin{cases} \rho_w \cdot \dfrac{\mathbf{r}+t_{go}\mathbf{v}}{\|\mathbf{r}+t_{go}\mathbf{v}\|} & \textit{Outside } \aleph \\ \|\mathbf{r}+t_{go}\mathbf{v}\| - m - \dfrac{1}{2}\Delta\rho\cdot t_{go}^2 = 0 & \text{Arbitrary in } \aleph \end{cases}$$

Demanding kinetic hit (m=0), one gets :

$$\bar{u}^* = \frac{2}{1-\frac{\rho_w}{\rho_v}}\cdot\frac{1}{t_{go}^2}\cdot(\bar{r}+t_{go}\bar{v}) \qquad \bar{w}^* = -\frac{2}{1-\frac{\rho_w}{\rho_v}}\cdot\frac{1}{t_{go}^2}\cdot(\bar{r}+t_{go}\bar{v}) \tag{1.11}$$

Polar Coordinates

Let $\mathbf{r} = \|r\|$ be the range between pursuer and evader, and λ is the LOS orientation relative to a fixed direction :

$$r = \begin{bmatrix} rcos(\lambda) \\ rsin(\lambda) \end{bmatrix} \cdot \backslash\frac{\partial}{\partial t} \quad \Rightarrow \quad \dot{r} = v = \begin{bmatrix} \dot{r}cos(\lambda) - r\dot{\lambda}sin(\lambda) \\ \dot{r}sin(\lambda) + r\dot{\lambda}cos(\lambda) \end{bmatrix} \tag{1.12}$$

Thus,

$$\|r\| = r^2 \tag{1.13}$$
$$\|v\| = \dot{r}^2 + r^2\dot{\sigma}^2 \tag{1.14}$$
$$r^T v = r\dot{r} \tag{1.15}$$

Plugging the polar coordinates in **Eq.** 1.10 and we get :

$$\left\|r + t_{go}v\right\|^2 = r^2 + (\dot{r}^2 + r^2\dot{\lambda}^2)t_{go}^2 + 2(r\dot{r})t_{go} = (m + \frac{1}{2}\Delta\rho t_{go}^2)^2 \tag{1.16}$$

Note that $\mathbf{u}^*$ is comprised of axial (u_r^*) and perpendicular (u_λ^*) components, and γ is the angle between LOS and the $(r + t_{go}v)$ vector. By so we get :

$$cos(\gamma) = \frac{r + t_{go}v}{\frac{1}{2}(\Delta\rho)t_{go}^2} \tag{1.17}$$
$$sin(\gamma) = \frac{r\dot{\sigma}}{\frac{1}{2}(\Delta\rho)t_{go}^2} \tag{1.18}$$

Optimal strategy pair $\{u^*, w^*\}$ in polar coordinates :

$$\mathbf{u}_r^* = \rho_u \cos(\gamma) = \rho_u \cdot \frac{r + t_{go}\dot{r}}{m + \frac{1}{2}\Delta\rho \cdot t_{go}^2} \qquad \mathbf{u}_\lambda^* = \rho_u \sin(\gamma) = \rho_u \cdot \frac{r\dot{\lambda}t_{go}}{m + \frac{1}{2}\Delta\rho \cdot t_{go}^2}$$

Demanding kinetic hit (m=0), one gets :

$$\mathbf{u}_r^* = \rho_u \cos(\gamma) = \rho_u \cdot \frac{r + t_{go}\dot{r}}{\frac{1}{2}\Delta\rho \cdot t_{go}^2} = \frac{2}{1 - \frac{\rho_w}{\rho_u}} \frac{1}{t_{go}^2} \cdot \left(r + t_{go}\dot{r}\right)$$

$$\mathbf{u}_\lambda^* = \rho_u \sin(\gamma) = \rho_u \cdot \frac{r\dot{\lambda}t_{go}}{\frac{1}{2}\Delta\rho \cdot t_{go}^2} = \frac{2}{1 - \frac{\rho_w}{\rho_u}} \cdot \frac{1}{t_{go}} \cdot r\dot{\lambda}$$

Note : Same goes identically for w^* but with $\rho_w = \sqrt{w_r^2 + w_\lambda^2}$.

Spherical Coordinates

Let us consider spherical approach in 3D space that satisfies :

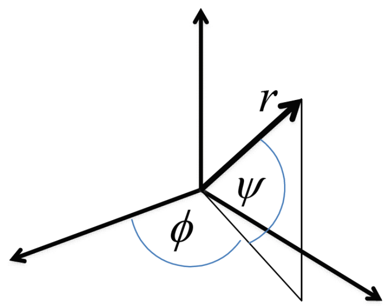

That is to say :

$$\mathbf{r} = \begin{bmatrix} r\cos\psi\cos\phi \\ r\cos\psi\sin\phi \\ r\cos\psi \end{bmatrix} \quad \cdot \backslash \frac{\partial}{\partial t} \quad \Rightarrow \quad \dot{\mathbf{r}} = \mathbf{v} = \begin{bmatrix} \dot{r}\cos\psi\cos\phi - \dot{\psi}r\sin\psi\cos\phi - \dot{\phi}r\cos\psi\sin\phi \\ \dot{r}\cos\psi\sin\phi - \dot{\psi}r\sin\psi\sin\phi + \dot{\phi}r\cos\psi\cos\phi \\ \dot{r}\cos\psi - r\sin\psi \end{bmatrix}$$

Optimal strategy pair $\{u^*, w^*\}$ in spherical coordinates :

$$\mathbf{u}_r^* = \rho_u \cdot \frac{r + t_{go}\dot{r}}{m + \frac{1}{2}\Delta\rho \cdot t_{go}^2} \qquad \mathbf{u}_\psi^* = \rho_u \cdot \frac{r\dot{\psi}}{m + \frac{1}{2}\Delta\rho \cdot t_{go}^2} \cdot t_{go} \qquad \mathbf{u}_\phi^* = \rho_u \cdot \frac{r\dot{\phi}\cos\psi}{m + \frac{1}{2}\Delta\rho \cdot t_{go}^2} \cdot t_{go}$$

Demanding kinetic hit (m=0), one gets :

$$\mathbf{u}_r^* = \frac{2}{1 - \frac{\rho_w}{\rho_u}} \frac{1}{t_{go}^2} \cdot \left(r + t_{go}\dot{r}\right) \qquad \mathbf{u}_\psi^* = \frac{2}{1 - \frac{\rho_w}{\rho_u}} \frac{1}{t_{go}} \cdot r\dot{\psi} \qquad \mathbf{u}_\phi^* = \frac{2}{1 - \frac{\rho_w}{\rho_u}} \frac{1}{t_{go}} \cdot r\dot{\phi}\cos\psi$$

2 Prove : Optimal Strategies and Optimal Cost

Writing down again the state space :

$$\dot{x} = \begin{bmatrix} \dot{r} \\ \dot{v} \end{bmatrix} = \begin{bmatrix} 0 & I_3 \\ 0 & 0 \end{bmatrix} \begin{bmatrix} r \\ v \end{bmatrix} + \begin{bmatrix} 0 \\ -I_3 \end{bmatrix} u + \begin{bmatrix} 0 \\ I_3 \end{bmatrix} w \tag{2.1}$$

Where,

$$\begin{aligned} \dot{x} = Ax + Bu + Cw \qquad & Dynamics \\ (u \leq \rho_u) \in U, \quad (w \leq \rho_w) \in W \qquad & Constraints \\ J = \|Mx(t_f)\| \qquad & Terminal\ Cost \end{aligned} \tag{2.2}$$

Define the Zero Effort Miss variable :

$$y = M\Phi(t_f, t)x = r + t_{go}v \quad where \quad \Phi(t_f, t) = e^{A \cdot t_{go}} = \begin{bmatrix} I & t_{go}I \\ 0 & I \end{bmatrix} \tag{2.3}$$

$$X(t_f, t) = M\Phi(t_f, t)B(t) = -t_{go}I \qquad Pursuer \tag{2.4}$$

$$Y(t_f, t) = M\Phi(t_f, t)C(t) = t_{go}I \qquad Evader \tag{2.5}$$

$$y = M\Phi x = r + t_{go}v \qquad ZEM \tag{2.6}$$

Using Transition Matrix property we get :

$$\begin{aligned} \dot{y} = X(t_f, t)u + Y(t_f, t)w = t_{go}(w - u) \\ since \quad \dot{\Phi}(t_f, t) = -\Phi(t_f, t)A(t) \end{aligned} \tag{2.7}$$

We'll define the following :

$$\nu(y, t) = \|y\| \tag{2.8}$$

$$W(t) \triangleq \nu \circ y(t) = \big\|y(t)\big\| \tag{2.9}$$

$$\Delta \triangleq \Delta_y \nu \cdot \dot{y} = \frac{y^T}{\|y\|}(w - u)t_{go} \tag{2.10}$$

The following optimal pair $\{u^*,\ w^*\}$ will minimize / maximize $\frac{\partial W}{\partial t}$ respectively by :

$$\frac{dW(t)}{dt} = \Delta^*(t) = (\rho_w - \rho_u) \cdot t_{go} = -\Delta\rho \cdot t_{go} \tag{2.11}$$

$$u^* = \rho_u \cdot \frac{y}{\|y\|} \qquad w^* = \rho_w \cdot \frac{y}{\|y\|} \tag{2.12}$$

Plugging each in **Eq.** 2.10, yields the saddle point inequality,

$$J(u^*, w) \leq J(u^*, w^*) \leq J(u, w^*) \tag{2.13}$$

$$Equivalently, \qquad \Delta(u^*, w) \leq \Delta(u^*, w^*) \leq \Delta(u, w^*) \tag{2.14}$$

$$\Delta(u^*, w) \leq \frac{y^T}{\|y\|}(\rho_u \cdot \frac{y}{\|y\|} - \rho_w \cdot \frac{y}{\|y\|})t_{go} \leq \Delta(u, w^*) \tag{2.15}$$

$$Simplifying, \qquad \Delta(u^*, w) \leq \Delta\rho t_{go} \leq \Delta(u, w^*) \tag{2.16}$$

Integrate the above,

$$J(u^*, w) \leq -\frac{1}{2}\Delta\rho t_{go}^2 + \big\|y(0)\big\| \leq J(u, w^*) \tag{2.17}$$

$$Hence, \qquad J^* = \big\|y(0)\big\| - \frac{1}{2}\Delta\rho t_{go}^2 \tag{2.18}$$

To conclude, we've proved the following,
Optimal Strategies - (**Eq.** 2.12)
Optimal Cost Function - (**Eq.** 2.18).

3 Kinematic Equations in Polar Coordinates

Reminder of the polar coordinates obtained at **Eq.** 1.12 :

$$r = \begin{bmatrix} rcos(\lambda) \\ rsin(\lambda) \end{bmatrix} \cdot \backslash\frac{\partial}{\partial t} \quad \Rightarrow \quad \dot{r} = v = \begin{bmatrix} \dot{r}cos(\lambda) - r\dot{\lambda}sin(\lambda) \\ \dot{r}sin(\lambda) + r\dot{\lambda}cos(\lambda) \end{bmatrix}$$

Another derivation yields :

$$r^T\ddot{r} = -r^2\dot{\lambda}^2 + r\ddot{r} = r\|\ddot{r}\|\,cos(r,\ddot{t}) \tag{3.1}$$

$$\tag{3.2}$$

We get a Non-Linear differential game such that **radial** controls becomes :

$$\ddot{r} - r\dot{\lambda}^2 = w_r - u_r \tag{3.3}$$

Similarly, we can extract **tangential** controls out of :

$$\|\ddot{r}\|^2 = (r\ddot{\lambda} + 2\dot{r}\dot{\lambda})^2 + (\ddot{r} - r\dot{\lambda}^2)^2 \quad \Rightarrow \quad r\ddot{\lambda} + 2\dot{r}\dot{\lambda} = w_\lambda - u_\lambda \tag{3.4}$$

Given the following constraints upon the controllers :

$$\|u\| \leq \rho_u \qquad \|w\| \leq \rho_w \tag{3.5}$$

$$where \qquad \rho_u > \rho_w \tag{3.6}$$

And respectively the cost function and the desired miss distance :

$$J = \big\|r(t_f)\big\| \qquad where \quad r(t_f) = y(t_f) \tag{3.7}$$

$$Therefore \qquad J = \big\|y(t_f)\big\| \tag{3.8}$$

Expressing the conflict is obtained by using optimal pair $\{u^*,\, w^*\}$ that satisfies the saddle point inequality regarding the miss distance. Projecting it onto polar coordinates yields non-linear kinematics.

4 Prove by contradiction : Non-Maneuvering Case

Let us assume **oppositely** that a *non-optimal* maneuvering target ($\tilde{w} \neq w^*$) has better performances over optimal one, and thus interceptor needs longer flight time to fulfil capture.

We get the following cost functions :

$$Optimal \qquad \tilde{J}(u^*, w^*) = \left\| y(t_f^*) \right\| = m \tag{4.1}$$

$$Non - Optimal \qquad \tilde{J}(u^*, \tilde{w}) = \left\| y(\tilde{t_f}) \right\| = m \tag{4.2}$$

$$Thus, \qquad \left\| y(t) \right\| \geq m \qquad \forall \qquad t \leq \tilde{t_f} \tag{4.3}$$

We've seen on (**Eq.** 2.13) that an **optimal** pair $\{u^*, w^*\}$ satisfy the saddle point inequality:

$$J(u^*, w) \leq J(u^*, w^*) = m \leq J(u, w^*) \tag{4.4}$$

$$respectively, \qquad J(u^*, \tilde{w}) \leq J(u^*, w^*) = m \leq J(u, w^*) \tag{4.5}$$

And thus we get

$$J(u^*, \tilde{w}) \leq J(u^*, w^*) = m \tag{4.6}$$

$$Hence, \qquad m < m \tag{4.7}$$

Which satisfies contradiction, using (**Eq.** 4.3).

5 Prove : Co-Linearity conditions of r and v at t_f

Let us assume optimal target maneuver, and examine the kinematic vectors when $t \simeq t_f$.

Firstly, define the angle between **r** and **v** as $\beta \triangleq \angle\,(\mathbf{r},\mathbf{v})$. Then we get,

$$r^T v = \|r\|\|v\| \cdot cos(\beta) \tag{5.1}$$

$$r\dot{r} = r\sqrt{\dot{r}^2 + r^2\dot{\lambda}^2} \cdot cos(\beta) \qquad \cdot \backslash(\quad)^2 \tag{5.2}$$

$$cos^2(\beta) = \frac{\dot{r}^2}{\dot{r}^2 + r^2\dot{\lambda}^2} \stackrel{?}{=} 1 \qquad \Leftrightarrow \qquad \beta = 0 \tag{5.3}$$

In order to clarify when $r^2\dot{\lambda}^2 \to 0$, we shall use **Eq.** 1.16 :

$$\left\|r + t_{go}v\right\|^2 = r^2 + (\dot{r}^2 + r^2\dot{\lambda}^2)t_{go}^2 + 2(r\dot{r})t_{go} = (m \quad + \quad \frac{1}{2}\Delta\rho t_{go}^2)^2$$

Assuming u^* maneuevers optimally (m=0) :

$$\left\|r + t_{go}v\right\|^2 = r^2 + (\dot{r}^2 + r^2\dot{\lambda}^2)t_{go}^2 + 2(r\dot{r})t_{go} = (\cancelto{0}{m} + \frac{1}{2}\Delta\rho t_{go}^2)^2 \tag{5.4}$$

$$(r + \dot{r}t_{go})^2 + (r\dot{\lambda}t_{go})^2 = (\frac{1}{2}\Delta\rho t_{go}^2)^2 \tag{5.5}$$

Extracting $r\dot{\lambda}$,

$$r\dot{\lambda}t_{go} = \sqrt{(\frac{1}{2}\Delta\rho t_{go}^2)^2 - (r + \dot{r}t_{go})^2} \tag{5.6}$$

$$r\dot{\lambda} = \sqrt{(\frac{1}{2}\Delta\rho t_{go})^2 - (\frac{r}{t_{go}} + \dot{r})^2} \tag{5.7}$$

$$\tag{5.8}$$

By bounding the condition, one gets,

$$r\dot{\lambda} = \sqrt{(\frac{1}{2}\Delta\rho t_{go})^2 - (\frac{r}{t_{go}} + \dot{r})^2} \leq (\frac{1}{2}\Delta\rho t_{go}) \tag{5.9}$$

Which at $t \to t_f$ satisfies,

$$r\dot{\lambda} = \frac{1}{2}\Delta\rho \cdot \cancelto{0}{t_{go}} = 0 \tag{5.10}$$

Plugging it back into (**Eq.** 5.3) one gets,

$$cos^2(\beta) = \frac{\dot{r}^2}{\dot{r}^2 + \cancelto{0}{(r\dot{\lambda})^2}} = \frac{\dot{r}^2}{\dot{r}^2} = 1 \qquad \Rightarrow \qquad \beta = 0^\circ,\ \ 180^\circ. \tag{5.11}$$

Let us depict the 2 obtained options at t_f of co-linearity conditions :

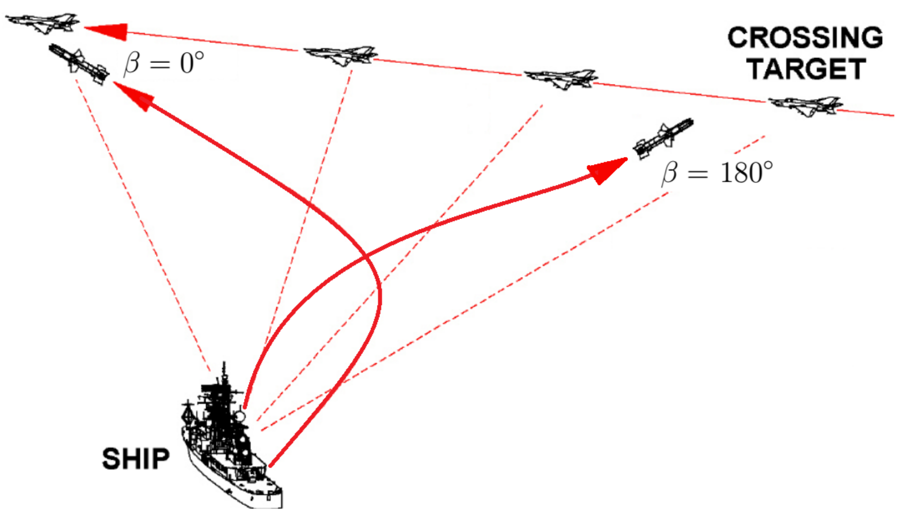

Figure 2: **Left :** Tail Chase **Right :** Head On

We therefore see that the target maneuver (w), bounded by its optimal maneuver (w^*), does not influence on **r, v** vectors at termination.

6 Planar Motion and Kinetic Hit Conditions

Let us assume the following initial conditions, assuming optimality (m=0):

$r_0 = 15$ [km], $\lambda_0 = 0$ $[rad]$, $\rho_u = 10$ $[g]$

$\dot{r}_0$= -1280 $[m \setminus s]$, $\dot{\lambda}_0 = 0.018$ $[rad \setminus s]$, $\rho_w = 5$ $[g]$.

Plugging into **Eq.** 1.12, we get :

$$r_0 = \begin{bmatrix} rcos(\lambda) \\ rsin(\lambda) \end{bmatrix} = \begin{bmatrix} 15,000 \\ 0 \end{bmatrix} [m] \tag{6.1}$$

$$\dot{r}_0 = v_0 = \begin{bmatrix} \dot{r}cos(\lambda) - r\dot{\lambda}sin(\lambda) \\ \dot{r}sin(\lambda) + r\dot{\lambda}cos(\lambda) \end{bmatrix} = \begin{bmatrix} -1,280 \\ 270 \end{bmatrix} [\frac{m}{sec}] \tag{6.2}$$

Let us assume Head-On collision as depicted in **Fig.** 2, where both vehicles are launched from ground level ($\lambda_0 = 0\ ^\circ$) and move towards each other. The dynamic *Simulink* system that would use us for expressing the trajectories in inertial coordinates would be as follows :

$$\boxed{\ddot{\mathbf{r}} = -\frac{\mathbf{r} + t_{go}\dot{\mathbf{r}}}{\frac{1}{2}t_{go}^2}}$$

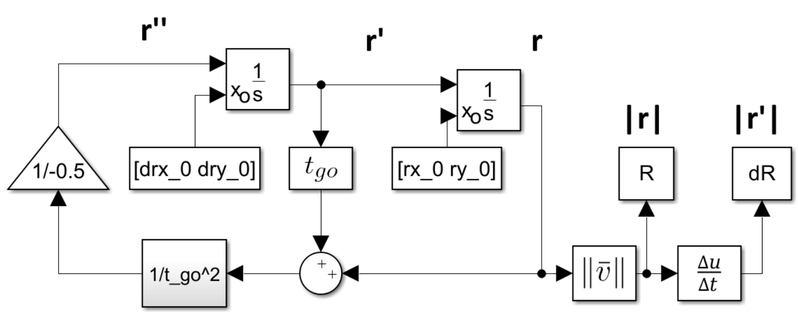

Figure 3: Vector Guidance Loop

The t_f duration is derived out of (**Eq.** 6.3)'s solution, and is a **minimal-real-positive** :

$$4th \quad order \quad Polynomial - \quad \frac{1}{4}\Delta\rho^2 t_{go}^4 - (\dot{r}^2 + r^2\dot{\lambda}^2)t_{go}^2 - 2(r\dot{r})t_{go} - r^2 = 0 \tag{6.3}$$

7 Optimal Trajectories ($\dot{\lambda} = 0.018$ [rad/s])

Solving (**Eq.** 6.3) froms few solutions, where 3 of them are **real-positive**. However, our **minimal** t_f solution when ($\dot{\lambda} = 0.018$) is $t_f = 11.13[sec]$:

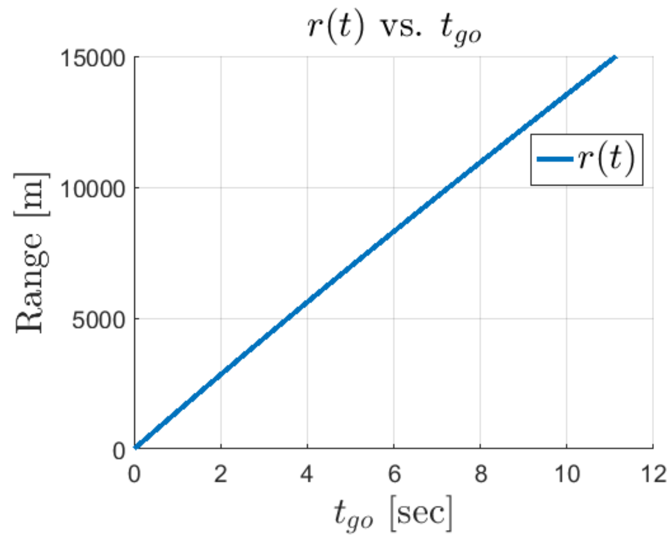

Figure 4: Range vs. t_{go}

The velocities vectors are increasing towards $t_{go} \to 0$:

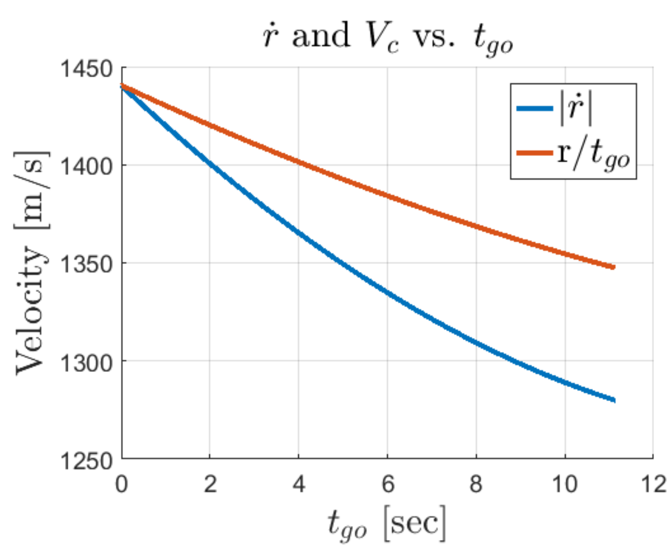

Figure 5: Range rate and Closing Velocity vs. t_{go}

Note : We get that $V_c > |\dot{r}|$, since it is derived out of (**Eq.** 6.3), unlike regular V_c at **PN**.

8 Optimal Trajectories ($\dot{\lambda} = 0.022$ [rad/s])

This time we get only one **real-positive** t_f when ($\dot{\lambda} = 0.022$), and is $t_f = 37.655$ $[sec]$:

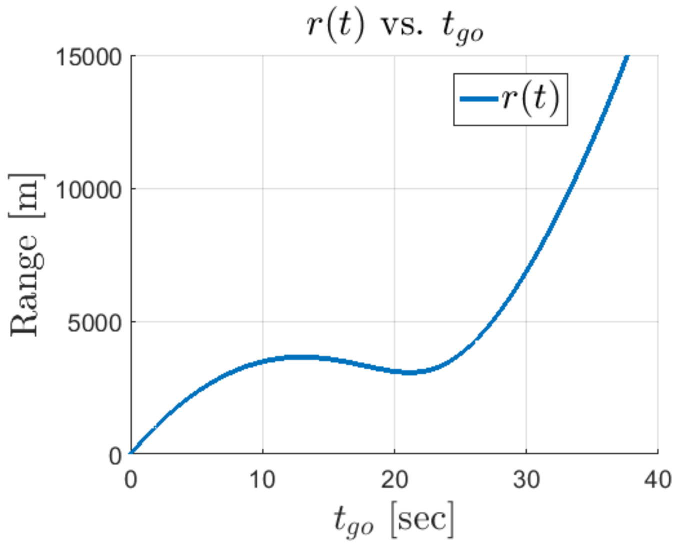

Figure 6: Range vs. t_{go}

Entirely different from previous section, where plots seemed monotonous, here the range and the velocities change direction / sign. The range has curvy form that creates local extremums along t_{go}. Neither do the velocities are monotonous, and temporarily $|\dot{r}|$ becomes negative.

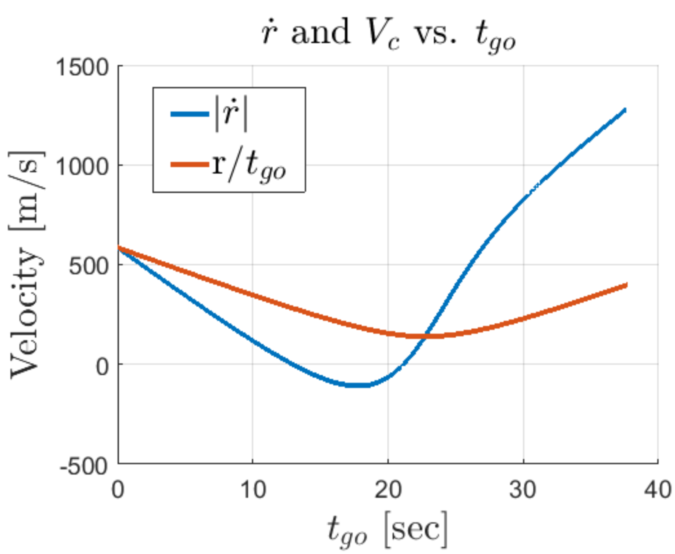

Figure 7: Range rate and Closing Velocity vs. t_{go}

9 Bifurcation

As seen on **Eq.** 1.16 the t_{go} equation is :

$$\left\|r + t_{go}v\right\| = m + \frac{1}{2}\Delta\rho t_{go}^2$$

As in **Eq.** 6.3, under optimal conditions (m=0), it is developed into :

$$\frac{1}{4}\Delta\rho^2 t_{go}^4 - (\dot{r}^2 + r^2\dot{\lambda}^2)t_{go}^2 - 2(r\dot{r})t_{go} - r^2 = 0$$

One would like to examine the tangency and the general interaction between both sides, . As mentioned in the course book, using *Sylvester Matrix* and then using the *resultant method*, the determinant product becomes :

$$\underline{\underline{4r^2\Delta\rho^4 - \Delta\rho^2\dot{r}^4 - 20r^2\Delta\rho^2\dot{r}^2\dot{\lambda}^2 + 8r^4\Delta\rho^2\dot{\lambda}^4 + 4\dot{r}^6\dot{\lambda}^2 + 12r^2\dot{r}^4\dot{\lambda}^4 + 12r^4\dot{r}^2\dot{\lambda}^6 + 4r^6\dot{\lambda}^8}} \quad (9.1)$$

This equation can be solved in numerous ways, depends on the subjected parameter. Here, let us examine the ($\dot{r}$,$\dot{\lambda}$) plane :

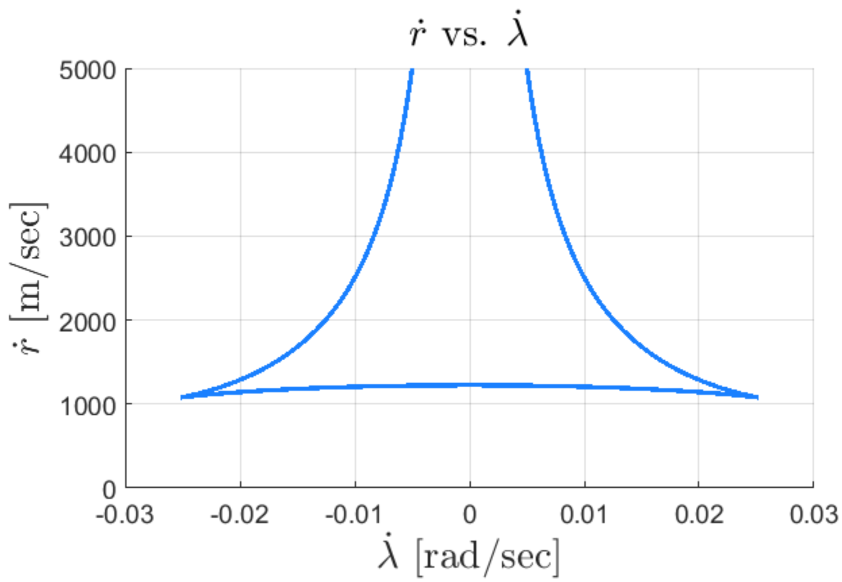

Figure 8: First-Pass Capture Zone

The blue lines are bounding the "First-Pass" zone in the domain $-0.0201 \leq \dot{\lambda} \leq 0.0201$. These initial conditions dictates a comfortable supremacy of the interceptor over the target, since it is "privileged" to return for a second pass, and improve the capture.

Inside zoom towards the base of the plot, shows an artificial part, that can be expanded towards the base dashed line. Outside and **above** that domain, the interceptor will be able to hit the target only once, on the **second pass**.

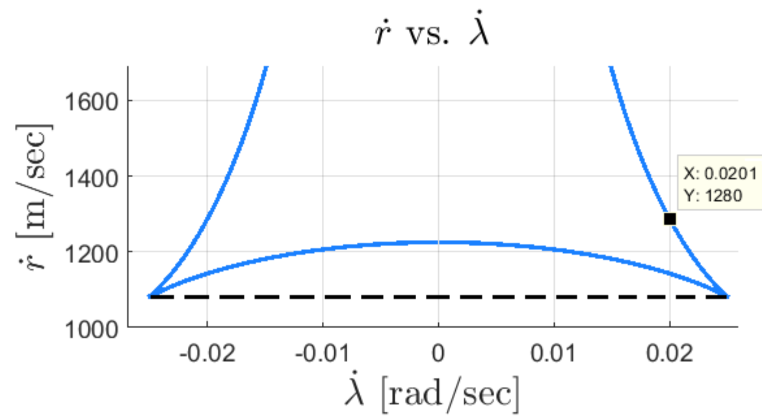

Figure 9: Resulting Curves that bound the First-Pass zone

Let us express the tangency of $r(t)$ under ($\dot{\lambda} \leq 0.0201$, $r = 15,000$ [m], $|\dot{r}| = 1280$ [m/sec]) :

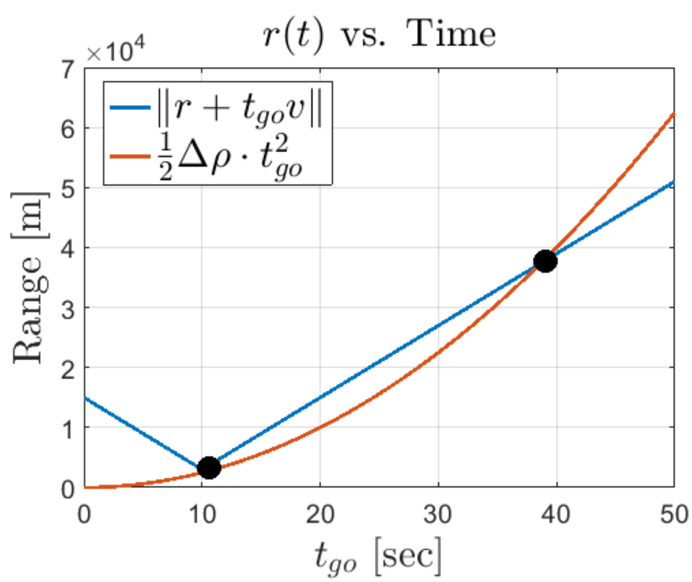

Figure 10: Tangency and t_{go} jump ($\dot{\lambda} = 0.02$) [rad/s])

Higher values ($\dot{\lambda} > 0.201$) would coerce the debated ”Jump”, hence getting only one tangency, on second pass. Otherwise ($\dot{\lambda} \leq 0.0201$), we get a pair of passes at different t_{go}'s.

The following schema shows the $f(t_{go}, \dot{\lambda})$ evolution when $|\dot{r}|$ grows steadily ($r = 15,000$ [m]):

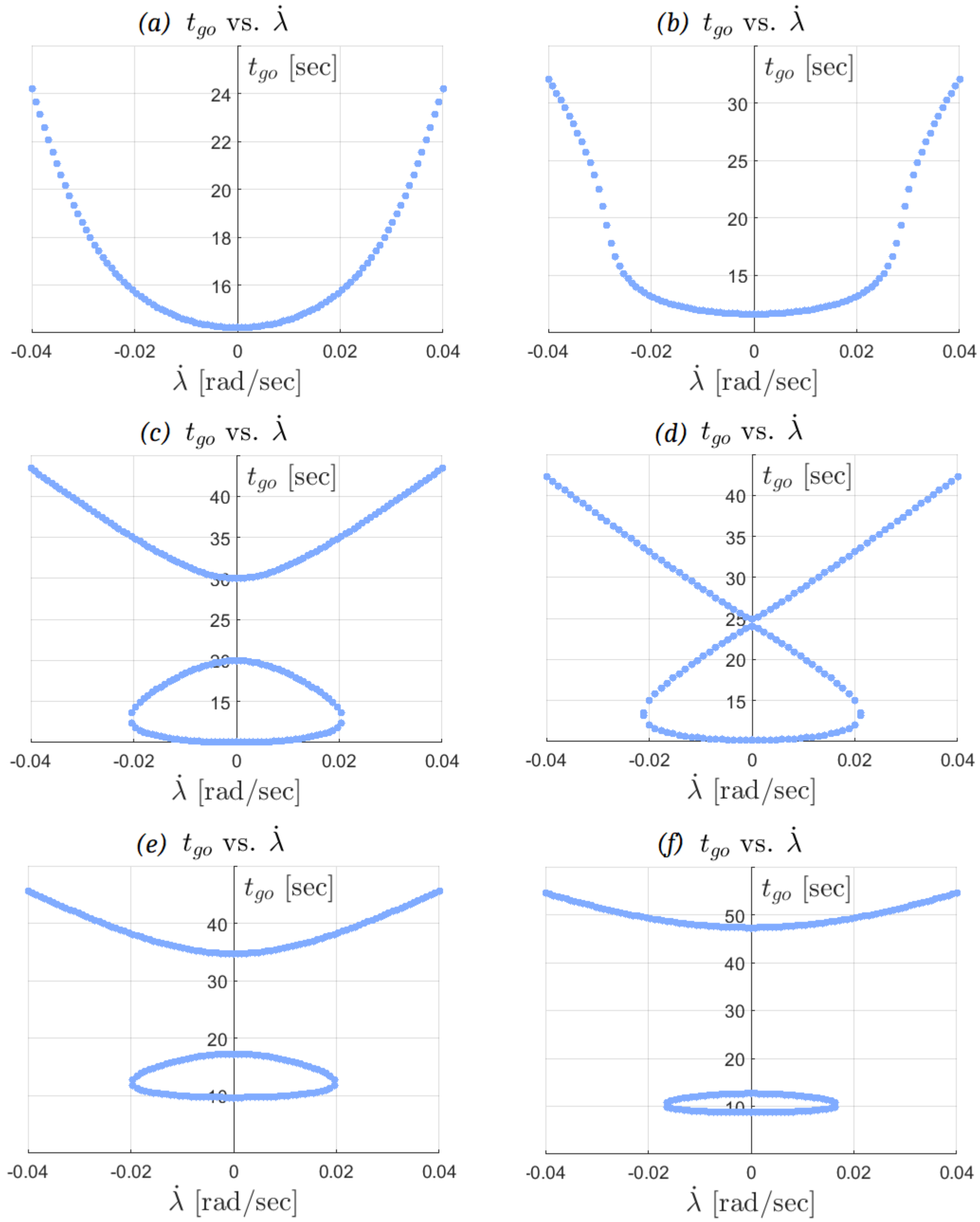

Figure 11: Discontinuous t_{go}

(i)	$\lvert\dot{r}\rvert$ [m/sec]	(i)	$\lvert\dot{r}\rvert$ [m/sec]
a	700	d	1250
b	1000	e	1300
c	1225	f	1500

10 Optimal r(t), v(t) Comparison

Expressing optimal controllers (m=0) :

$$Pursuer \quad u^* = \rho_u \cdot \frac{r + t_{go}v}{\left\| r + t_{go}v \right\|} \qquad Evader \quad w^* = \rho_w \cdot \frac{r + t_{go}v}{\left\| r + t_{go}v \right\|} \tag{10.1}$$

The state variable is then :

$$\ddot{r} = \underline{\underline{w^* - u^*}} = -\Delta\rho \cdot \frac{r + t_{go}v}{\left\| r + t_{go}v \right\|} = -\Delta\rho \cdot \frac{r + t_{go}v}{\frac{1}{2}\Delta\rho t_{go}^2} = -\frac{r + t_{go}v}{\frac{1}{2}t_{go}^2} \tag{10.2}$$

We get the 2nd ODE:

$$t_{go}^2\ddot{r}(t_{go}) - 2t_{go}\dot{r}(t_{go}) + 2r(t_{go}) \qquad i.c. \quad r(t_f) = r_0, \qquad \dot{r}(t_f) = -v_0 \tag{10.3}$$

$$r(t_{go}) = c_1 \cdot t_{go}^2 + c_2 \cdot t_{go} \qquad Substituting \quad i.c. \quad and \quad t_{go} = t_f - t \tag{10.4}$$

We get the optimal expressions :

$$r(t) = \frac{(t_f - t)[(t_f + t)r_0 + (t_f \cdot t)v_0]}{t_f^2} \qquad \cdot \backslash \frac{\partial}{\partial t} \tag{10.5}$$

$$\dot{r}(t) = \frac{2t \cdot r_0 - t_f(t_f - 2t)v_0}{t_f^2} \tag{10.6}$$

Using the initial conditions obtained at (**Eq.** 6.1, 6.2), we will check the optimal trajectories under $\dot{\lambda} = 0.018, 0.022$ [rad/s].

Hereby is the *Matlab* code used for optimal trajectories :

```
% ------------------- Define t as symbolic variable ------------------- %
syms t real
r_t  = (  (tf-t)*((tf+t)*r + (tf*t)*dr')  )/tf^2; %  R(t) - symbolic
dr_t = (     (2*t)*r - tf*(tf-2*t)*dr'    )/tf^2;    % dR(t) - symbolic
% ----------- Inline Function - Allows Plugging vectors ----------- %
R_t   = inline( norm(r_t) );
dR_t  = inline( norm(dr_t) );
T = linspace(0, tf)';
```

r(t), v(t) Comparison @ $\dot{\lambda} = 0.018$ [rad/s]

Let's simulate the optimal trajectories at (**Eq.** 10.5), and compare with **section 7** results :

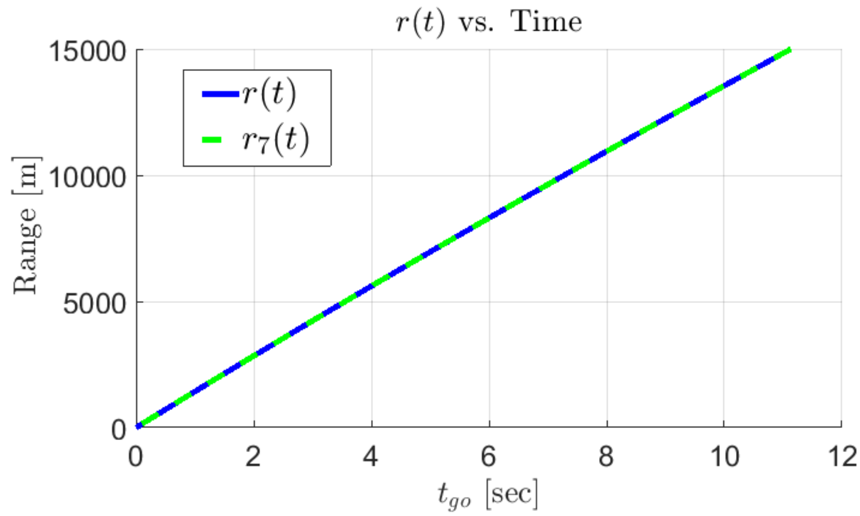

Figure 12: Range vs. t_{go}

No difference can be seen between both simulations. Now, let's check the velocities graphs :

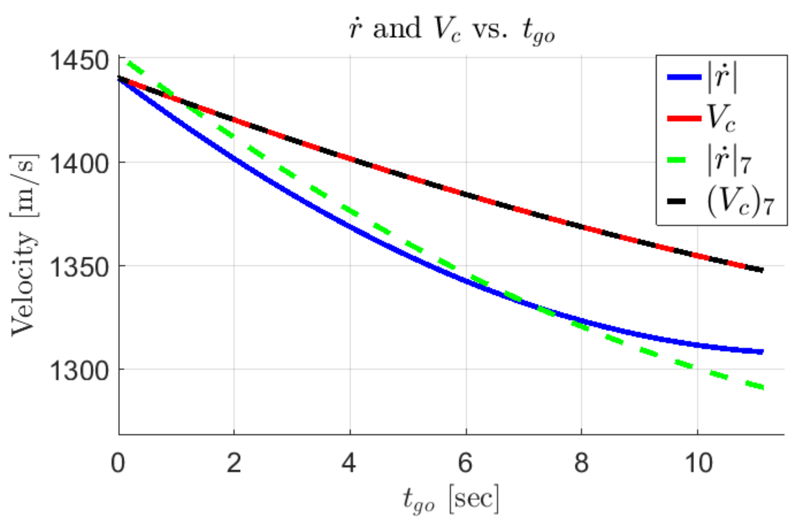

Figure 13: Closing Velocity t_{go}

Here the results seem slightly different. Although both V_c's converge, $|\dot{r}|_7$ exhibits different trajectories. The problem stems from the fact that $|\dot{r}_7(0)| = \sqrt{(-1280)^2 + (270)^2}$ on *Simulink* (**Eq.** 6.2), while analytic $|\dot{r}(t)|$ at (**Eq.** 10.5) satisfies $|r(t = 0)| = 1280$.

r(t), v(t) Comparison @ $\dot{\lambda} = 0.022$ [rad/s]

Either here do the curves converge, exhibiting local minima and maxima along $\bar{r}(t)$:

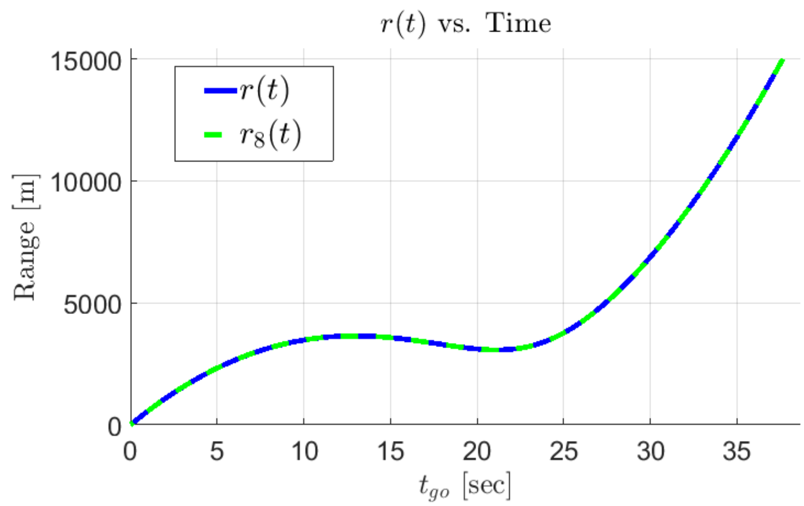

Figure 14: Range vs. t_{go}

V_c's converge as well, since both $\bar{r}(t)$'s converge, and it's calculated by their fraction :

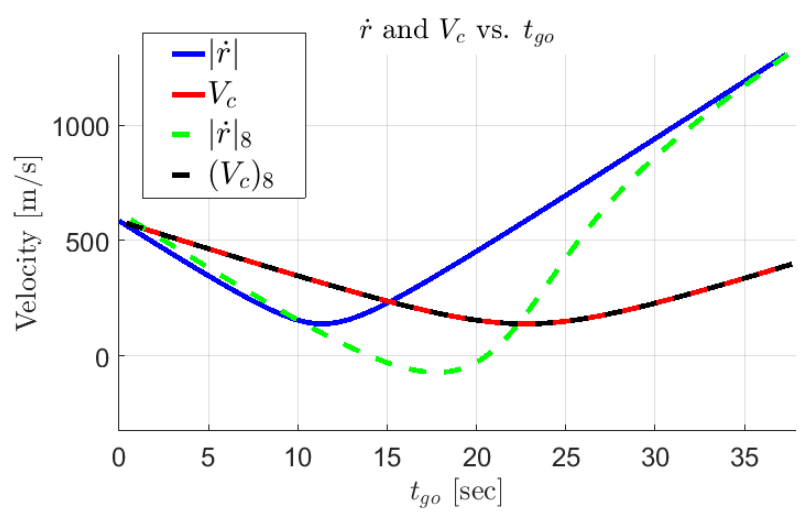

Figure 15: Closing Velocity t_{go}

However, $\dot{\bar{r}}(t)$ exhibits rather different policy along flight time. As already explained above (**Fig.** 7), the derived velocity may become negative for a short period. But here (**Eq.** 10.5), when $\dot{\bar{r}}(t)$ is analytically expressed, negativity depends exclusively on initial conditions.

11 Initial Conditions for $|\dot{r}(t)| < 0$

One may ask what is the explanation for the $\dot{r}_8$ being negative ?

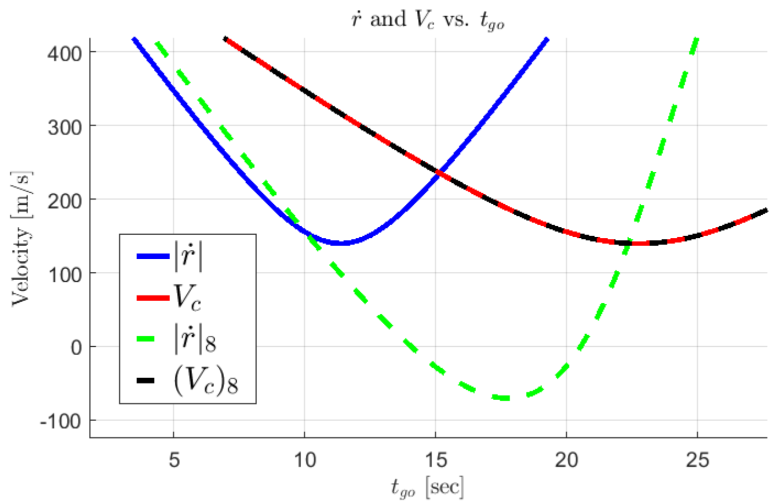

Figure 16: Closing Velocity t_{go}

As seen on **Fig.** 8, the boundaries of the first pass satisfy $\dot{\lambda} \leq 0.201$. Once passing these values, the interceptor is "Jumping" for its next "Window of Opportunity", which is the next (**Eq.** 6.3) **real-positive** root.

By so, the interceptor might have already passed the target, meaning that now it is needed to **turn around** and try re-hitting once again - 2nd pass. The negative zone $(-\dot{r}) < 0$ is after the 1st pass, when vehicles have just passed and are moving away from each other. Its duration is the time taken to complete a full turn around.

Analytically speaking, using **Eq.** 5.3 we get :

$$r\dot{r} = r\sqrt{\dot{r}^2 + r^2\dot{\lambda}^2} \cdot cos(\beta) \quad \cdot \backslash (r^{-1})^2 \quad \Rightarrow \quad \dot{r} = \sqrt{\dot{r}^2 + r^2\dot{\lambda}^2} \cdot cos(\beta) \tag{11.1}$$

One can tell that $\dot{r}$ sign is dependant exclusively on $cos(\beta)$ sign. Therefore :

$$(-\dot{r}) < 0 \qquad \forall \qquad \underline{\underline{|\beta| > 90^\circ}} \tag{11.2}$$

12 Thrust Inclination

Let us look at the planar geometry depicted relative to the inertial reference :

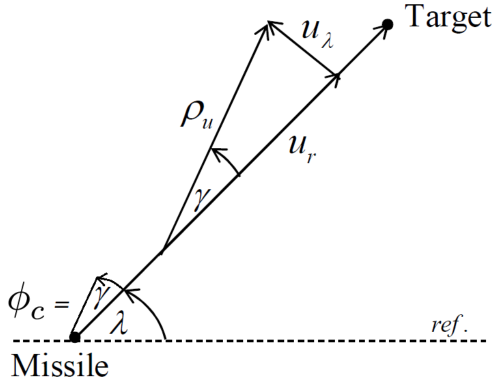

Figure 17: Thrust Inclination - Planar Geometry

The thrust inclination command is given by $\phi_c = \gamma + \lambda$:

$$\phi_c = \lambda + arcsin(\frac{u_\lambda}{\rho_u}) = \lambda + arcsin\left(\frac{\rho_u sin(\gamma)}{\rho_u}\right) = \lambda + arcsin\left(\frac{r \cdot \dot{\lambda}}{\frac{1}{2}\Delta\rho \cdot t_{go}}\right) \quad (12.1)$$

$$Denote: \qquad \dot{\lambda}_{cr} = \frac{r}{\frac{1}{2}\Delta\rho \cdot t_{go}} \quad \Rightarrow \quad \phi_c = \lambda + arcsin(\frac{\dot{\lambda}}{\dot{\lambda}_{cr}}) = \lambda + arcsin(\frac{2V_c\dot{\lambda}}{\Delta\rho}) \quad (12.2)$$

Let us build compatible *Simulink* diagram to simulate the **MP** and **NMP** performances :

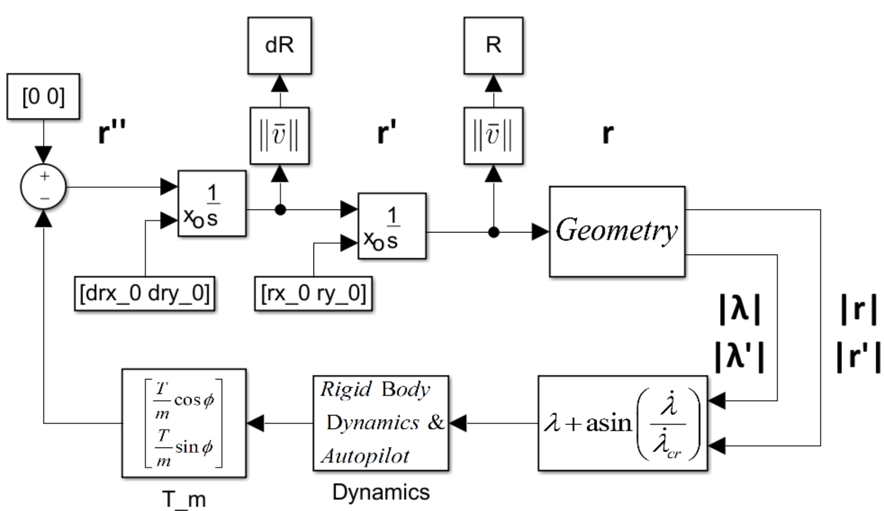

Figure 18: Thrust Inclination - Planar Guidance

The 2 admissible configurations of the Thrust Inclination method are as follows :

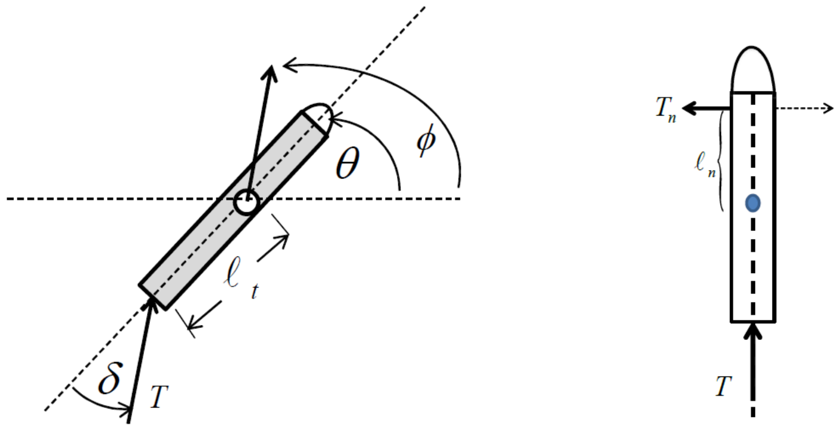

Figure 19: **Left :** TVC **Right :** NJC

Similarly to **Project 1** where we analysed the missile's configurations (**MP, NMP**), either here does it work the same :

$$\underline{\underline{TVC}}: \qquad assuming: \quad M_\delta = \frac{Tl_j}{I}$$
$$I\ddot{\theta} = -T \cdot sin(\delta) \cdot l_t \quad \Rightarrow \quad \ddot{\theta} \cong -M_\delta \cdot \delta \tag{12.3}$$
$$\underline{\underline{NCJ}}: \qquad assuming: \quad \delta = \frac{T_n}{T}$$
$$I\ddot{\theta} = T_n \cdot \delta l_n \quad \Rightarrow \quad \ddot{\theta} \cong M_\delta \cdot \delta \tag{12.4}$$

The Auto-Pilot dynamic realization will be either same here :

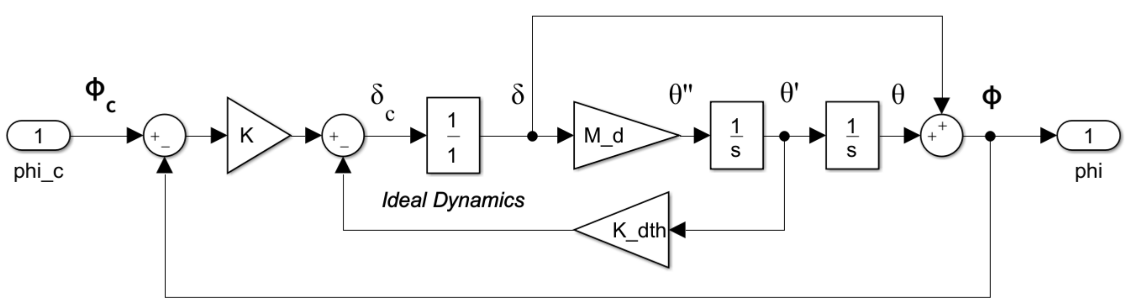

Figure 20: The Auto-Pilot Dynamics

Simulations

Running the 2 configurations (**MP, NMP**), we get a quite similar results at both dynamics:

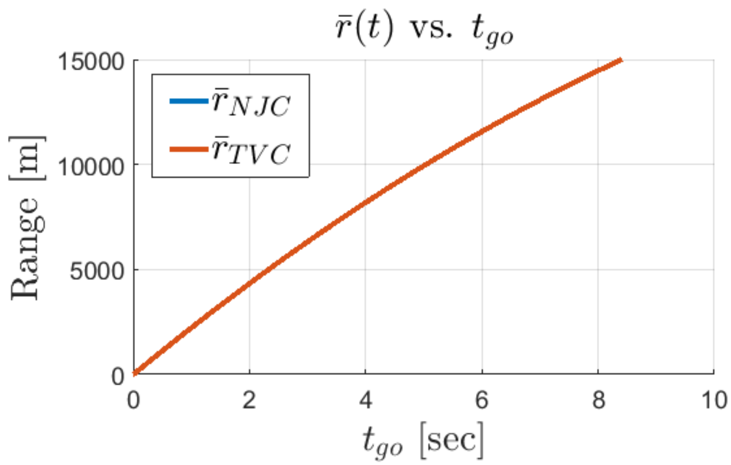

Figure 21: Thrust Inclination - Range vs. t_{go}

We can see a rather convergence of the trajectories, little influenced by the phase sign. However, in the close-up we can watch the slight differences regarding the miss distance :

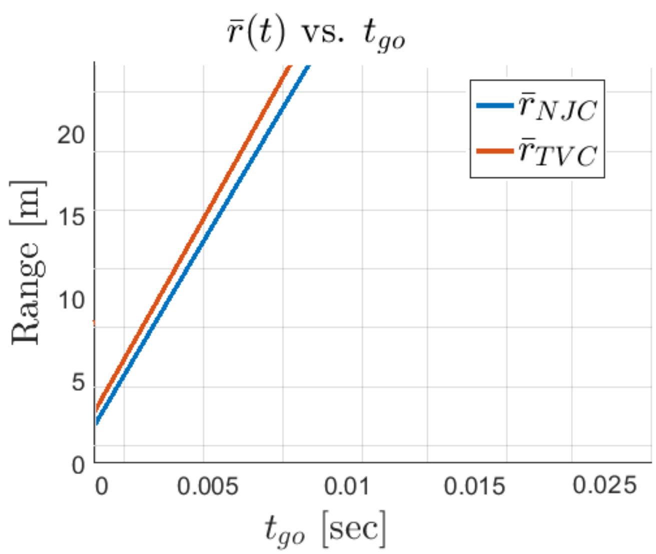

Figure 22: Thrust Inclination - Range vs. t_{go} (Zoom-In)

As expected, the **MP** (NCJ) performances are slightly better, getting $y(t_f)_n = 2.035[m]$ as opposed to the **NMP** (TVC) $y(t_f)_t = 3.880[m]$.

Chapter B - 3D Exo-Atmospheric Interception, LQ Controllers

13 LQ Vector Guidance

The following developments are based on the paper : "Exo-Atmospheric Interception via Linear Quadratic Optimization / Shaul Gutman".

Under ideal conditions and non-maneuvering target, $\mathbf{x} = [\text{ r} \quad \text{v }]^T$ satisfies the state space :

$$\dot{x} = Ax + Bu + C\cancelto{0}{v} \; ; \quad Respectively : \tag{13.1}$$

$$\dot{x} = \begin{bmatrix} 0 & I_3 \\ 0 & 0 \end{bmatrix} x + \begin{bmatrix} 0 \\ -I_3 \end{bmatrix} u \tag{13.2}$$

The cost function is then (**k** - control effort) :

$$J = \left\| \bar{M} \cdot \bar{x}(t_f)^2 \right\| + \int_0^{t_f} k\|\bar{u}\|\, dt \quad where \quad M = [I_3 \quad 0]^T \tag{13.3}$$

After order reduction we get :

$$J = \left\| y(t_f) \right\|^2 + \int_0^{t_f} k\|\bar{u}\|\, dt \tag{13.4}$$

$$Optimal \quad Control : \qquad u^* = -k^{-1} X^T(t_f, t) P(t) y \tag{13.5}$$

$$where \quad -\dot{P} = -k^{-1} X X^T P^T \quad and \quad P(t_f) = I \tag{13.6}$$

Using Riccati Equation, as further presented in the essay, one gets :

$$u_r^* = \frac{t_{go}}{k + t_{go}^3/3} \cdot (r + t_{go}\dot{r}) \qquad and \qquad u_\lambda^* = \frac{t_{go}^3}{k + t_{go}^3/3} \cdot (\frac{r}{t_{go}})\dot{\lambda} \tag{13.7}$$

When control effort is nullified ($\mathbf{k} \to 0$), one gets :

$$u_r^* = \frac{3}{t_{go}^2} \cdot (r + t_{go}\dot{r}) \qquad and \qquad u_\lambda^* = 3 \cdot (\frac{r}{t_{go}})\dot{\lambda} \tag{13.8}$$

14 Prove : Constant Direction of u^* in Inertial Frame

Given non-maneuvering target, the state vector satisfies :

$$\ddot{r} = w^* - u^* = -u_r^* = \frac{3}{t_{go}^2} \cdot (r + t_{go}\dot{r}) \tag{14.1}$$

$$2nd \quad ODE \qquad t_{go}^2\ddot{r} + 3t_{go}\dot{r} + 3r = 0 \tag{14.2}$$

$$(dt_{go} = -dt) \quad \Rightarrow t_{go}^2\ddot{r} - 3t_{go}\dot{r} + 3r = 0 \tag{14.3}$$

$$i.c. \qquad r(t_f) = r_0, \quad \dot{r}(t_f) = -v_0 \tag{14.4}$$

Solvable by Euler Equation :

$$r(t_{go}) = c_1 t_{go}^3 + c_2 t_{go} \quad Plugging \quad i.c. \tag{14.5}$$

Using Matlab solver :

$$r(t) = \frac{t_f - t}{2t_f^2} \cdot [3t_f^3(r_0 + v_0 t_f) - 2v_0 t_f^3 - (t_f - t)^2(r_0 + v_0 t_f)] \tag{14.6}$$

And now plug inside the ZEM expression :

$$\bar{y} = \bar{r} + t_{go}\bar{v} = \frac{(t_f - t)^3}{t_f^3} \cdot (r_0 + v_0 t_f) \tag{14.7}$$

$$\bar{u}^* = \frac{3(t_f - t)}{t_f^3} \cdot (\bar{r}_0 + \bar{v}_0 t_f) \tag{14.8}$$

As seen above, u^* faces **constant** direction along the flight time, and its magnitude **decays** linearly towards $t \to t_f$.

15 Analyse the Jump phenomenon and its meaning

Considering **Eq.** 9.1, under **LQ Guidance** where $\Delta\rho = \frac{2}{3}u_m$:

$$f(t_{go}) = (\frac{u_m}{3})^2 t_{go}^4 - (\dot{r}_0^2 + (r_0\dot{\lambda})^2)t_{go}^2 - 2(r_0\dot{r}_0)t_{go} - r_0^2 \tag{15.1}$$

$$f'(t_{t_{go}}) = 4(\frac{u_m}{3})^2 t_{go}^3 - 2(\dot{r_0}^2 + (r_0\dot{\lambda})^2)t_{go} - 2(r_0\dot{r_0}) \tag{15.2}$$

That function's curves on the $(\dot{\lambda}, \dot{r})$ plane, bound the admissible set of points that ensure interception by 1st pass, when both sides are most close. Hence $t \to t_f$:

$$f(t_f) = (\frac{u_m}{3})^2 t_f^4 - (\dot{r_0}^2 + (r_0\dot{\lambda})^2)t_f^2 - 2(r_0\dot{r_0})t_f - r_0^2 \tag{15.3}$$

$$f'(t_f) = 4(\frac{u_m}{3})^2 t_f^3 - 2(\dot{r_0}^2 + (r_0\dot{\lambda})^2)t_f - 2(r_0\dot{r_0}) \tag{15.4}$$

Let us plot **Eq.** 15.3 numerically ($r_0 = 15,000$ $[m]$, $\dot{r}_0 = -1280$ $[m/s]$, $u_m = 100$ $[m/s^2]$):

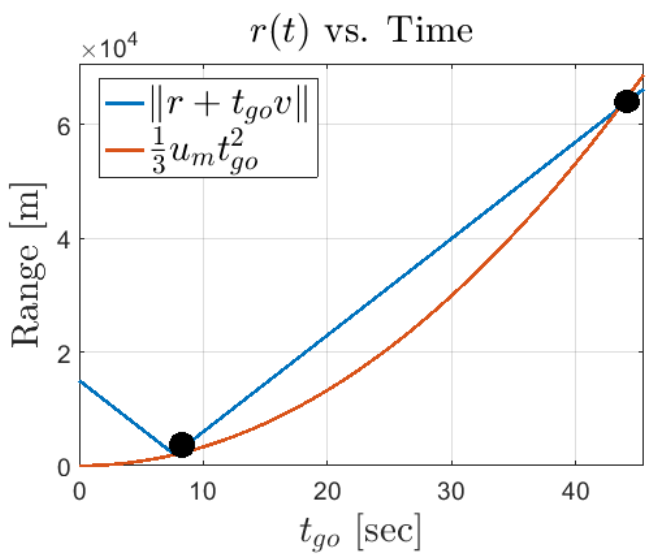

Figure 23: Jump in LQ Guidance

Like in **Fig.** 10, we can see that minor violation of **Eq.** 15.3's initial conditions, might cause the Jump **out** of the 1st pass capture zone. The 2 bold circles denote the tangency points, whereas the interceptor's t_f might jump from 1st pass to 2nd pass.

Let us mind the $(\dot{\lambda}, \dot{r})$ surface that bounds the sensitive i.c. between 1st pass and 2nd pass. As seen in the bifurcation at **section 9** :

$$4r^2\Delta\rho^4 - \Delta\rho^2\dot{r}^4 - 20r^2\Delta\rho^2\dot{r}^2\dot{\lambda}^2 + 8r^4\Delta\rho^2\dot{\lambda}^4 + 4\dot{r}^6\dot{\lambda}^2 + 12r^2\dot{r}^4\dot{\lambda}^4 + 12r^4\dot{r}^2\dot{\lambda}^6 + 4r^6\dot{\lambda}^8 = 0$$

$$LQ \quad Guidance \quad \Downarrow \quad \Delta\rho = \frac{2}{3}u_m \quad \Downarrow$$

$$\underline{\underline{16u_m^4 r_0^2 - 9u_m^2\dot{r}_0^4 - 180u_m^2 r_0^2\dot{r}_0^2\dot{\lambda}^2 + 72u_m^2 r_0^4\dot{\lambda}^4 + 81\dot{r}_0^6\dot{\lambda}^2 + 243r_0^2\dot{r}_0^4\dot{\lambda}^4 + 243r_0^4\dot{r}_0^2\dot{\lambda}^6 + 81r_0^6\dot{\lambda}^8}}$$

Solving numerically ($r_0 = 15,000$ $[m]$) :

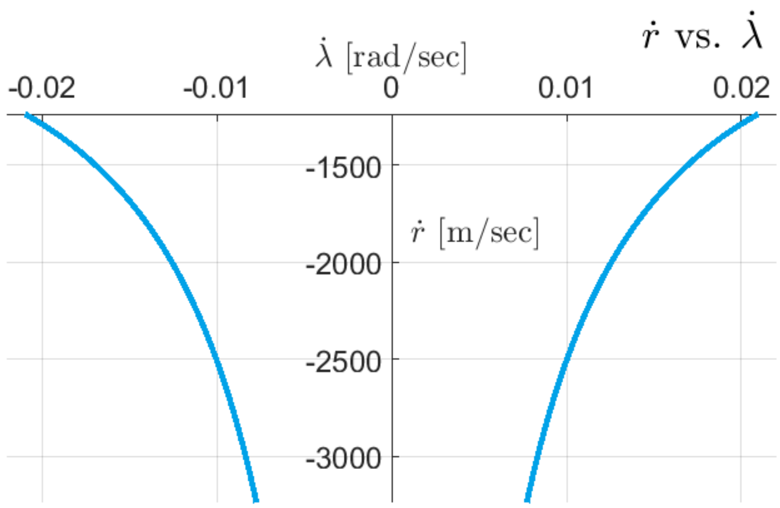

Figure 24: LQ Guidance - Jump Surface

When approaching physical capture $(r \to 0)$, the equation decays into :

$$-9u_m^2\dot{r}_0^4 + 81\dot{r}_0^6\dot{\lambda}^2 = 0 \quad \Rightarrow \quad \dot{\lambda}^2 = \frac{9u_m^2\dot{r}_0^4}{81\dot{r}_0^6} \tag{15.5}$$

And 1st pass capture is guaranteed under :

$$\underline{\underline{|\dot{\lambda}| < \frac{u_m}{3|\dot{r}|}}} \tag{15.6}$$

16 LQ Guidance - Simulations ($m_r = 1[m]$, $u_m = 100[m/s^2]$)

Unlike previously (**Eq.** 1.16), the control effort now **is not** nullified ($k \neq 0$) :

$$\ddot{r} = -u_r^* = -\frac{t_{go}}{k + t_{go}^3/3} \cdot (r + t_{go}\dot{r}) \tag{16.1}$$

$$2nd \quad ODE: \qquad (3k + t_{go}^3)\ddot{r} + 3t_{go}^2\dot{r} + 3r = 0 \tag{16.2}$$

$$(dt_{go} = -dt) \quad \Rightarrow \quad (3k + t_{go}^3)r'' - 3t_{go}^2 r' + 3r = 0 \tag{16.3}$$

$$r(t_{go}) = c_1 t_{go}^3 + c_2 t_{go} + c_3 \tag{16.4}$$

$$i.c. \qquad r(t_f) = r_0, \quad \dot{r}(t_f) = v_0 \tag{16.5}$$

So finally we get :

$$y(t) = \frac{(3k + t_{go}^3)}{(3k + t_f^3)}(r_0 + t_f v_0) \tag{16.6}$$

And the i.c. given now **include** miss distance ($m_r \neq 0$),

$$\|y(t_f)\| = m_r = \frac{3k}{3k + t_f^3}\|r_0 + t_f v_0\| \tag{16.7}$$

$$Respectively \qquad \|u^*\| = u_m = \frac{3t_f}{3k + t_f^3}\|r_0 + t_f v_0\| \tag{16.8}$$

Division of both gives us the relation :

$$k = \frac{m_r t_f}{u_m} \tag{16.9}$$

Which will plugged at each run. However, the initial conditions stay the same as before :

$$\bar{r}_0 = [15,000 \quad 0] \quad [m] \qquad \dot{\bar{r}}_0 = [-1280 \quad 0] \quad [m/s]$$
$$m_r = 1 \quad [m] \qquad u_m = 100 \quad [m/s^2]$$

In order to get a slight "feeling" of the control effort **k**'s influence, I will run several simuation with a set of miss distances, that would yield respectively ($t_f = 22.341$):

$$m_r = [0.0001 \ 0.1 \ 1 \ 100] \ [\text{m}] \qquad \Rightarrow \qquad k = [0.00002 \ 0.0223 \ 0.2234 \ 22.3410]$$

Using the following *Simulink* diagram :

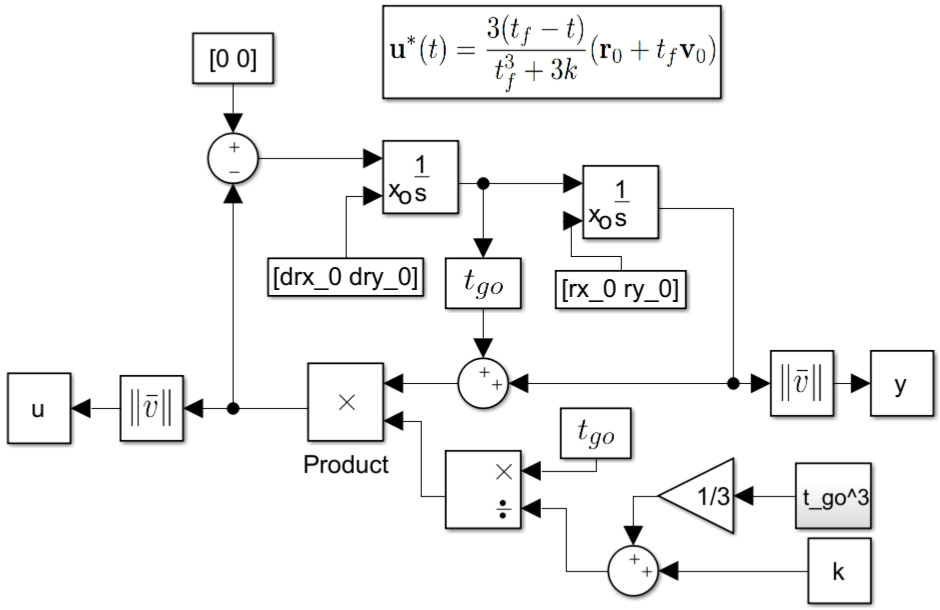

Figure 25: LQ Guidance System

We get the range graph :

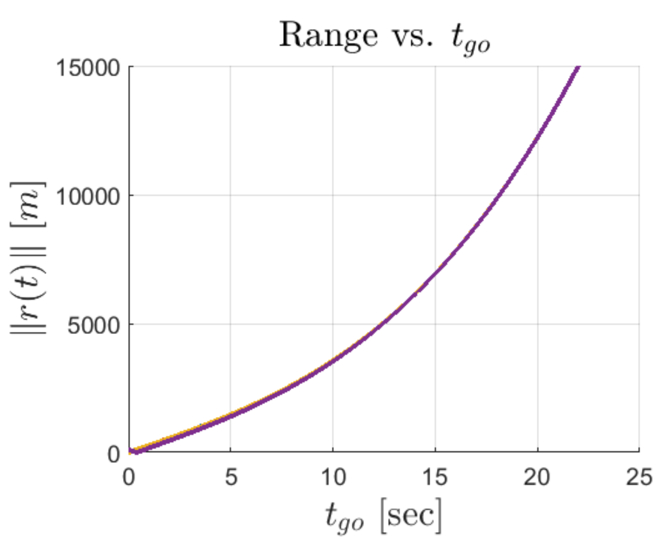

Figure 26: LQ Guidance - Range

Where no acute difference seems out the different k's effort.

The same goes here for the optimal acceleration $u(t)$:

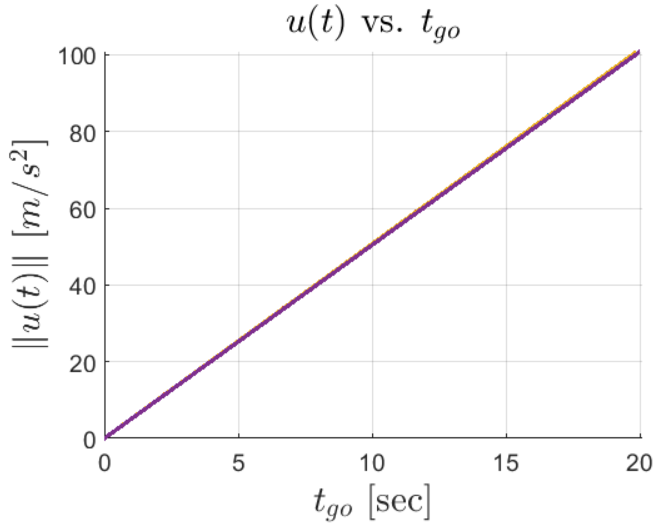

Figure 27: LQ Guidance - $u(t)$

Either here can we see a steadily decrease of u towards zero. However, giving a close-up look on the miss distance we would witness slight difference resulting from the weight of k :

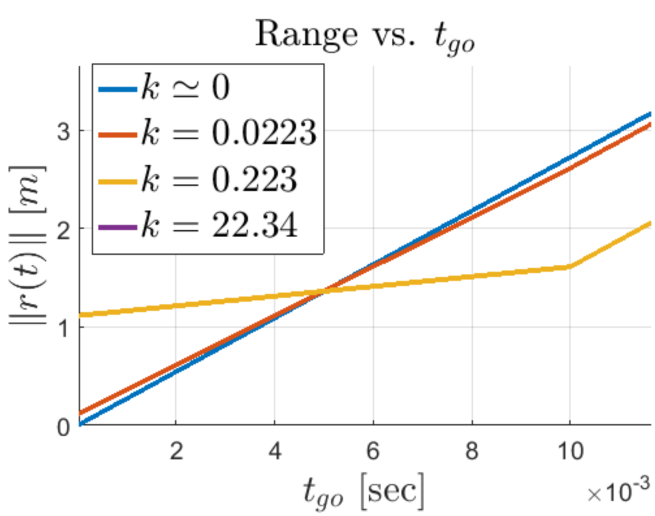

Figure 28: LQ Guidance - Miss Distance

We can see that when $k \simeq 0$ the miss distance equals zero, expressing optimality. But when increasing its weight, so does miss grows.

$-fin-$